

Performance Evaluation of Wireless Communication Systems over Composite α – μ /Gamma Fading Channels

Osamah S. Badarneh¹

Published online: 16 June 2017
© Springer Science+Business Media New York 2017

Abstract The composite α – μ /gamma distribution is considered in this paper. Specifically, we derived closed-form expressions for the power probability density function (PDF) and the cumulative density function (CDF). We then use the PDF and the CDF to derive novel closed-form expressions for the outage probability, the average symbol error rate, and the average channel capacity over the composite α – μ /gamma fading channels. All derived expressions are valid for integer and non-integer values of the fading parameters. Some representative numerical examples are provided to study the impact of the fading and shadowing parameters on the system performance. Furthermore, the numerical results are compared with Monte-Carlo simulations. Both results demonstrate excellent agreement which validates our analysis.

Keywords Composite fading channels · Long-term fading · Performance analysis · Short-term fading

1 Introduction

Composite fading channels are introduced for modeling the mixture of fading (short-term fading) and shadowing (long-term fading) in wireless communication systems. The short-term fading represents the fluctuation in the received signal during a very short duration. On the other hand, the long-term fading represents the fluctuation in the received signal during a longer duration than the one associated with the short-term fading. In the literature, there are several models that characterize the short-term fading, as well as, the long-term fading in wireless channels. The Rice, the Rayleigh, the Nakagami- m and the Weibull distributions are examples of short-term fading [1]. Whereas, the gamma and log-normal

✉ Osamah S. Badarneh
obadarneh@ut.edu.sa

¹ Electrical Engineering Department, Faculty of Engineering, University of Tabuk, P.O. Box 741, 71491 Tabuk, Saudi Arabia

are examples of long-term fading. However, in some environments the short-term fading and the long-term fading can be occurred concurrently; thus, in this cases, the aforementioned channels are incapable to model these environments. This motivates the researchers for proposing new wireless channels models that take into consideration this phenomena. The Rayleigh-lognormal distribution, which is a mixture of the Rayleigh and lognormal distributions, was proposed for modelling fading-shadowing wireless channels [2]. In the same context, Raghavan developed a model for spatially correlated radar clutter. This model is a mixture of Rayleigh and gamma distributions and is known as the K -distribution [3]. It is shown that the K -distribution can be used to accurately model the Rayleigh-lognormal distribution [4]. Yilmaz and Alouini [5] introduced a new composite channel model known as extended generalized- K (EGK). The EKG models the fading in wireless millimeter wave (mmWave) channels and free-space optical (FSO) environments.

Performance analysis of wireless communication systems over different fading channels has gained much attention in the literature [6–16]. The author in [6] derived simple expression for the PDF of the received power of the gamma/gamma distribution, where the derived probability density function (PDF) is obtained by incorporating the Nakagami- m and the gamma distributions to model the fading and the shadowing, respectively. The authors in [7] studied the performance of an M -ary Phase Shift Keying (M -PSK) wireless communication system that operates over the α - η - μ fading channels perturbed by Laplacian noise. The performance is studied in terms of the average bit error rate (BER) under a new type of detector, known as minimum euclidian distance (MED) detector. In [8], the performance of maximal ratio combining (MRC) over a composite shadowed fading channels, known as the generalized- K distribution, is analyzed. In addition, the authors considered the effect of the co-channel interference (CCI) on the system performance. The authors in [9] derived exact expressions for the average symbol error probability (SEP) for various M -ary modulation schemes over Rician-Nakagami fading channels. In [10], closed-form expression for the moment generating function (MGF) in Weibull fading channels is obtained. Then based on the derived MGF expression, the symbol error rate for M -PSK is analyzed. In [11], H. Lee provided high signal-to-noise ratio (SNR) approximate closed-form expressions for the average error probabilities of several M -ary modulation schemes over Nakagami- q (so-called Hoyt) fading channels. The performance of an equal gain combiner (EGC) operating over Generalized- K (K_G) fading channels is analyzed and evaluated in [12]. The system performance is analyzed in terms of the outage probability, the average SEP, the amount of fading, and the average capacity. Jiayi et al. [13] analyzed the performance of a digital communication system that operates over the η - μ /gamma fading channels. The authors derived expressions -in terms of infinite sum of Meijer's G-function- for the average BER, outage probability, and average channel capacity. Ansari et al. [14] derived closed-form expressions for the PDF and the cumulative density function (CDF) of the sum of independent but not necessarily identically distributed (i.n.i.d.) gamma random variables. Then based on the PDF and CDF, the performance of the average BER and outage probability is analyzed. Stamenović et al. investigated the performance of wireless communication over α - η - μ fading channels subjected to co-channel interference. The system performance was analyzed in terms of the outage probability and the average BER [15].

Recently, Sofotasios have derived analytical expressions for the envelope PDF of different non-linear composite fading channels such as the α - κ - μ /gamma, α - κ - μ Extreme/gamma, κ - μ /gamma, κ - μ Extreme/gamma, and α - μ /gamma distributions [16]. However, the envelope PDF for the α - μ /gamma is valid only for integer values of the

fading parameter α . In addition, Sofotasios did not further elaborate on the performance analysis of wireless communication systems over the α - μ /gamma fading channels.

In this paper, we derived novel closed-form expression for the envelop PDF of the α - μ /gamma, which is valid for integer and non-integer values of the fading parameters. In addition, closed-form expressions for the envelop CDF, MGF, outage probability, average symbol error rate (SER), and average channel capacity over the composite α - μ /gamma are derived. Note that special cases for several fading distributions, such as gamma/gamma, Weibull/gamma, Nakagami- m /gamma, and Rayleigh/gamma distributions can be also obtained using our analytical results. Based on our analytical results, we then analyze the performance of a wireless communication system that operates over the α - μ /gamma.

The rest of the paper is organized as follows. The next section describes the composite α - μ /gamma fading distributions. Section 3 presents mathematical derivations for several performance metrics. In Sect. 4, we provide some numerical results and Monte-Carlo simulations. Besides, it provides discussions on the obtained results. Finally, Sect. 5 concludes the paper.

2 Composite α - μ /Gamma

The α - μ distribution describes the small-scale variation of the fading signal in a non-line-of-sight environment. The α - μ distribution is a general fading distribution that includes other well-known fading distributions such as the Weibull, the Nakagami- m , and their inclusive ones as special cases. The Weibull distribution can be obtained when $\mu = 1$, whereas Nakagami- m is obtained when $\alpha = 2$ and $\mu = m$.

The corresponding power PDF of the α - μ distribution is given by [17, Eq. (1)] as

$$f_X(x) = \frac{\alpha\mu^\mu}{\Gamma(\mu)\Omega^{\alpha\mu}} x^{\alpha\mu-1} \exp\left(-\frac{\mu}{\Omega^\alpha} x^\alpha\right), \quad (1)$$

where $\alpha > 0$ denotes the nonlinearity of the propagation medium and $\mu \geq 1/2$ is the number of the multi-path in each clusters.

The shadowing effect can be modeled as a gamma random variable (r.v.). As such, the PDF of a gamma r.v. is given in [18] as

$$f_Y(y) = \frac{1}{\Gamma(k)v^k} y^{k-1} e^{-y/v} \quad (2)$$

where $v = \mathbb{E}\{y\}/k$ is the scale parameter, k is the shape parameter of the gamma distribution, and $\mathbb{E}\{\cdot\}$ is the expectation operator.

2.1 The Power PDF of the Composite α - μ /Gamma Distribution

In order to consider the large-scale effects (i.e., path-loss and shadowing effects), we assume that the distance between the transmitter (Tx) and the receiver (Rx) is denoted by D and the path-loss exponent is denoted by δ (where $2 \leq \delta \leq 6$). Therefore, the entire channel response is a product of the small- and large-scale fading coefficients. The large-scale effects is represented by y/D^δ , where quantity D^δ describes how quickly the wave attenuates as a function of distance D .

Now, the overall instantaneous power of the received signal can be expressed as $\rho \triangleq z/D^\delta$, where $z = xy$. Therefore, to find the PDF of ρ , we need first to obtain the PDF of the product of the two random variables x and y . As such, the product of two random variables $z = xy$ can be given as

$$f_Z(z) = \int_0^\infty f_X(x)f_Y\left(\frac{z}{x}\right)\frac{1}{x}dx. \tag{3}$$

Now, to obtain the PDF $f_Z(z)$ of the composite α - μ /gamma distribution, we insert (1) and (2) into (3). Consequently, we obtain

$$f_Z(z) = \mathcal{A}z^{k-1} \int_0^\infty x^{2\mu-k-1} \exp\left(-\frac{z}{v}x^{-1}\right) \exp\left(-\frac{\mu}{\Omega^x}x^x\right)dx, \tag{4}$$

where $\mathcal{A} = \frac{\alpha\mu^k}{\Gamma(\mu)\Gamma(k)\Omega^{2\mu}v^k}$. To the best authors' knowledge the integral in (4) has not been reported before. As such, to solve this integral, we represent the exponential functions in terms of Fox's H-function using the identities [19, Eqs. (8.4.3.2)/(8.4.1.21)] and [20, Eq. (2.9.4)], thus (4) becomes

$$f_Z(z) = \frac{\mathcal{A}}{\alpha}z^{k-1} \int_0^\infty x^{2\mu-k-1}H_{1,0}^{0,1}\left[\frac{v}{z}x \middle| \begin{matrix} (1, 1) \\ - \end{matrix}\right] H_{0,1}^{1,0}\left[\frac{\mu^{1/x}}{\Omega}x \middle| \begin{matrix} - \\ (0, 1/\alpha) \end{matrix}\right]dx. \tag{5}$$

With the help of [19, Eq. (2.25.1.1)], then the PDF of $f_Z(z)$, in (5), can be expressed in a closed-form as

$$f_Z(z) = \frac{\mathcal{A}}{\alpha} \left(\frac{1}{v}\right)^{\alpha\mu-k} z^{\alpha\mu-1} H_{0,2}^{2,0}\left[\frac{\mu^{1/\alpha}}{v\Omega}z \middle| \begin{matrix} - \\ \left(0, \frac{1}{\alpha}\right), (k - \alpha\mu, 1) \end{matrix}\right], \tag{6}$$

where $H_{u,v}^{s,t}[\cdot | \bar{\quad}]$ is the well-known Fox's H-function [19, Eq. (8.3.1.1)]. Note that an accurate implementation of the Fox's H-function is outlined in [14]. Finally, the PDF of ρ (where $\rho = z/D^\delta$) can be obtained using random variable transformation, identity [20, Eq. (2.1.5)], and after some basic simplifications as

$$f_\rho(\rho) = \frac{1}{\Gamma(\mu)\Gamma(k)\rho} H_{0,2}^{2,0}\left[\frac{\mu^{1/\alpha}D^\delta}{v\Omega}\rho \middle| \begin{matrix} - \\ \left(\mu, \frac{1}{\alpha}\right), (k, 1) \end{matrix}\right]. \tag{7}$$

In case of gamma/gamma distribution, we note that the it can be obtained via the α - μ distribution in (1) by setting $\alpha = 1$, $\mu = \beta$, and $\Omega = \beta v$. As such, using (7) then the PDF of the gamma/gamma distribution, with the help of [20, Eq. (2.9.19)], can be expressed as

$$f_\rho(\rho) = \frac{2}{\Gamma(\beta)\Gamma(k)} \left(\frac{D^\delta}{v\beta}\right)^{\frac{k+\beta}{2}} \rho^{\frac{k+\beta}{2}-1} K_{k-\beta}\left(2\sqrt{\frac{D^\delta}{v\beta}}\rho\right) \tag{8}$$

where $K_\mu(\cdot)$ is the modified Bessel function of the second kind [21, Eq. (8.432)].

2.2 The Power CDF of the Composite α - μ /Gamma Distribution

The power CDF of the composite α - μ /gamma distribution can be obtained using the main definition of the CDF, that is

$$F_\rho(\rho) = \int_0^\rho f_\rho(\zeta) d\zeta, \tag{9}$$

where $f_\rho(\cdot)$ is given in (7).

Substituting (7) into (9) and with the aid of [22, Eq. (2.53)] and [20, Eq. (2.1.5)], then a closed-form expression for the CDF of the composite α - μ /gamma fading channels is obtained as

$$F_\rho(\rho) = \frac{1}{\Gamma(\mu)\Gamma(k)} H_{1,3}^{2,1} \left[\frac{\mu^{1/\alpha} D^\delta}{v\Omega} \rho \left| \begin{matrix} (1, 1) \\ \left(\mu, \frac{1}{\alpha}\right), (k, 1), (0, 1) \end{matrix} \right. \right]. \tag{10}$$

For gamma/gamma distribution, (10) simplifies to

$$F_\rho(\rho) = \frac{1}{\Gamma(\beta)\Gamma(k)} G_{1,3}^{2,1} \left[\frac{D^\delta}{v\nu} \rho \left| \begin{matrix} 1 \\ \beta, k, 0 \end{matrix} \right. \right], \tag{11}$$

where $G_{u,v}^{s,t}[\cdot | _]$ is the univariate Meijer's G-function [19, Eq. (8.2.1.1)]. Note that the Meijer's G-function is implemented in most standard software packages such as MATHEMATICA and MATLAB.

2.3 The MGF of the Composite α - μ /Gamma Distribution

The moment generating function (MGF) of ρ can be obtained by substituting (7) into (12)

$$\mathcal{M}(s) = \int_0^\infty f_\rho(\rho) e^{-s\rho} d\rho, \tag{12}$$

and then using [19, Eq. (2.25.2.3)], that is

$$\mathcal{M}(s) = \frac{1}{\Gamma(\mu)\Gamma(k)} H_{1,2}^{2,1} \left[\frac{\mu^{1/\alpha} D^\delta}{v\Omega s} \left| \begin{matrix} (1, 1) \\ \left(\mu, \frac{1}{\alpha}\right), (k, 1) \end{matrix} \right. \right]. \tag{13}$$

For gamma/gamma distribution, (13) reduces to

$$\mathcal{M}(s) = \frac{1}{\Gamma(\beta)\Gamma(k)} G_{1,2}^{2,1} \left[\frac{D^\delta}{v\nu s} \left| \begin{matrix} 1 \\ \beta, k \end{matrix} \right. \right]. \tag{14}$$

3 Performance Analysis

3.1 Outage Probability

The outage probability over the composite α - μ /gamma fading channels can be computed with the help of (10), that is

$$P_{out} = \Pr\{\rho < \rho_{th}\} = F_{\rho}(\rho_{th}), \tag{15}$$

where $\Pr\{\rho < \rho_{th}\}$ represents the probability that the power of the received signal is less than a predefined threshold ρ_{th} . With the aid of (10), the outage probability over the composite α - μ /gamma is given as

$$P_{out} = \frac{1}{\Gamma(\mu)\Gamma(k)} H_{1,3}^{2,1} \left[\frac{\mu^{1/\alpha} D^{\delta} \rho_{th}}{v \Omega} \middle| \begin{matrix} (1, 1) \\ \left(\mu, \frac{1}{\alpha}\right), (k, 1), (0, 1) \end{matrix} \right]. \tag{16}$$

For gamma/gamma distribution, (16) becomes

$$P_{out} = \frac{1}{\Gamma(\beta)\Gamma(k)} G_{1,3}^{2,1} \left[\frac{D^{\delta}}{v v} \rho_{th} \middle| \begin{matrix} 1 \\ \beta, k, 0 \end{matrix} \right]. \tag{17}$$

3.2 Amount of Fading

The amount of fading (AF) in wireless communication systems is given in [23] as

$$AF = \frac{\mathbb{E}[\rho^4] - (\mathbb{E}[\rho^2])^2}{(\mathbb{E}[\rho^2])^2} = \frac{\mathbb{E}[\rho^4]}{(\mathbb{E}[\rho^2])^2} - 1. \tag{18}$$

The AF in (18) can be obtained from the n th moment of ρ , which is defined as

$$\mathbb{E}[\rho^n] = \int_0^{\infty} \rho^n f_{\rho}(\rho) d\rho. \tag{19}$$

Inserting (7) in (19) and using [19, Eq. (2.25.2.1)], then the n th moment of the composite α - μ /gamma can be expressed as

$$\mathbb{E}[\rho^n] = \left(\frac{\mu^{1/\alpha} D^{\delta}}{v \Omega} \right)^{-n} \frac{\Gamma(\mu + \frac{n}{\alpha}) \Gamma(k + n)}{\Gamma(\mu) \Gamma(k)}. \tag{20}$$

From (18) and (20), AF can be expressed as

$$AF = \frac{\Gamma(\mu + \frac{4}{\alpha}) \Gamma(k + 4) \Gamma(\mu) \Gamma(k)}{[\Gamma(\mu + \frac{2}{\alpha}) \Gamma(k + 2)]^2} - 1. \tag{21}$$

Special Cases:

- (1) The gamma/gamma distribution: Using the identity [21, Eq. (8.331.1)], then (21) reduces to

$$AF = \frac{(\beta + 2)(\beta + 3)(k + 2)(k + 3)}{\beta k(\beta + 1)(k + 1)} - 1 \tag{22}$$

(2) The Nakagami-*m*/gamma distribution:

$$AF = \frac{(m + 1)(k + 2)(k + 3)}{mk(k + 1)} - 1 \tag{23}$$

(3) The Rayleigh/gamma distribution:

$$AF = \frac{2(k + 2)(k + 3)}{k(k + 1)} - 1 \tag{24}$$

3.3 Bit Error Rate Analysis

3.3.1 Coherent Modulation Schemes

For a large number of coherent modulation schemes, the conditional bit error rate over an AWGN can be written as [1]

$$P_b(e|\rho) = \psi Q(\theta\sqrt{\rho}) = \frac{\psi}{2\sqrt{\pi}} H_{1,2}^{2,0} \left[\frac{\theta^2}{2} \rho \left| \begin{matrix} (1, 1) \\ (0, 1), \left(\frac{1}{2}, 1\right) \end{matrix} \right. \right], \tag{25}$$

Note that (25) follows after using the relation between the complementary error function $\text{erfc}(x)$ and the Gaussian Q-function, $2Q(x) = \text{erfc}(x/\sqrt{2})$, and with the help of [19, 8.4.14.2] and [19, Eq. (8.3.2.21)]. The constant ψ and θ depends on the type of the modulation scheme. For example, for BPSK: $\psi = 1, \theta = \sqrt{2}$, for BFSK: $\psi = 1, \theta = 1$, for 4-QAM and QPSK: $\psi = 2, \theta = 1$, and for *M*-PAM: $\psi = 2(1 - \frac{1}{M}), \theta = \sqrt{\frac{6}{M^2-1}}$.

With the help of (25), the average BER for several coherent modulation schemes operating over a fading channel can be expressed as

$$P_b(e) = \frac{\psi}{2\sqrt{\pi}} \int_0^\infty f_\rho(\rho) H_{1,2}^{2,0} \left[\frac{\theta^2}{2} \rho \left| \begin{matrix} (1, 1) \\ (0, 1), \left(\frac{1}{2}, 1\right) \end{matrix} \right. \right] d\rho. \tag{26}$$

For the α - μ /gamma fading channels, substituting (7) into (26) and using [19, Eq. (2.25.1.1)], then the average BER can be obtained in a closed-form as

$$P_b(e) = \frac{\psi}{2\sqrt{\pi}\Gamma(\mu)\Gamma(k)} H_{2,3}^{2,2} \left[\frac{2\mu^{1/2} D^\delta}{v\theta^2} \frac{1}{\Omega} \left| \begin{matrix} (1, 1), \left(\frac{1}{2}, 1\right) \\ \left(\mu, \frac{1}{\alpha}\right), (k, 1), (0, 1) \end{matrix} \right. \right]. \tag{27}$$

For gamma/gamma distribution, (27) simplifies to

$$P_b(e) = \frac{\psi}{2\sqrt{\pi}\Gamma(\beta)\Gamma(k)} G_{2,3}^{2,2} \left[\frac{2D^\delta}{v\theta^2} \middle| \begin{matrix} 1, \frac{1}{2} \\ \beta, k, 0 \end{matrix} \right]. \tag{28}$$

3.3.2 Non-coherent Modulation Schemes

The average BER for non-coherent modulation schemes such as, BFSK, DBPSK, and *M*-FSK can be obtained by substituting (7) into (29)

$$P_b(e) = \varphi \int_0^\infty f_\rho(\rho) e^{-\phi\rho} d\rho, \tag{29}$$

and then using [19, Eq. (2.25.2.3)], that is

$$P_b(e) = \frac{\varphi}{\Gamma(\mu)\Gamma(k)} H_{1,2}^{2,1} \left[\frac{\mu^{1/\alpha} D^\delta}{v\Omega\phi} \middle| \begin{matrix} (1, 1) \\ \left(\mu, \frac{1}{\alpha}\right), (k, 1) \end{matrix} \right], \tag{30}$$

where φ and ϕ depend on type of modulation scheme. In case of non-coherent BFSK: $\varphi = \frac{1}{2}$ and $\phi = \frac{1}{2}$, DBPSK: $\varphi = \frac{1}{2}$ and $\phi = 1$, and for *M*-FSK: $\varphi = \frac{M-1}{2}$ and $\phi = \frac{1}{2}$.

For gamma/gamma distributions, (30) reduces to

$$P_b(e) = \frac{\varphi}{\Gamma(\beta)\Gamma(k)} G_{1,2}^{2,1} \left[\frac{D^\delta}{v\phi} \middle| \begin{matrix} 1 \\ \beta, k \end{matrix} \right]. \tag{31}$$

3.4 Ergodic Capacity

The average channel capacity can be obtained by averaging the capacity of an additive white Gaussian noise (AWGN) $\mathcal{C}_{\text{AWGN}} = \log_2(1 + \rho)$ over the instantaneous received power ρ , that is

$$\mathcal{C} = \int_0^\infty f_\rho(\rho) \log_2(1 + \rho) d\rho = \frac{1}{\ln 2} \int_0^\infty f_\rho(\rho) \ln(1 + \rho) d\rho. \tag{32}$$

Plugging (7) into (32) and representing the logarithm function $\ln(1 + \rho)$ in terms of Fox’s H-function using [19, Eq. (8.4.6.5)/(8.3.2.21)], then with the help of [19, Eq. (2.25.1.1)] the average capacity over the composite α - μ /gamma can be obtained in closed-form as

$$\begin{aligned} \mathcal{C} &= \frac{1}{\Gamma(\mu)\Gamma(k) \ln 2} \\ &\times H_{4,2}^{1,4} \left[\frac{v}{\mu^{1/\alpha} D^\delta} \Omega \middle| \begin{matrix} (1, 1), (1, 1), \left(1 - \mu, \frac{1}{\alpha}\right), (1 - k, 1) \\ (1, 1), (0, 1) \end{matrix} \right]. \end{aligned} \tag{33}$$

For gamma/gamma distribution, (33) becomes

$$\mathcal{C} = \frac{1}{\Gamma(\beta)\Gamma(k) \ln 2} G_{4,2}^{1,4} \left[\frac{v\Omega}{D^\delta} \middle| \begin{matrix} 1, 1, 1 - \beta, 1 - k \\ 1, 0 \end{matrix} \right]. \tag{34}$$

4 Numerical and Simulation Results

This section is devoted to analyze the system performance in terms of the outage probability, average BER, and ergodic channel (average channel) capacity. In addition, the influence of the path-loss and shadowing effects, as well as the fading parameters, on the aforementioned performance metrics is studied. Our numerical results obtained from (10), (27) and (33) are verified through Monte-Carlo simulations. Both results are in excellent agreement over a wide range of SNR values and for several values of the fading parameters, which validates our analysis.

Figure 1 depicts the effect of the shaping parameter k on the outage probability. The other fading parameters are set to: $\alpha = 1.25$, $\mu = 1$, $\nu = 2$, $\delta = 2$, $k = 4$, and $\gamma_{th} = 2$ dB. It is obvious that as k increases, the outage probability improves. This because as k increases, the scaling fading conditions decreases and thus better performance is expected.

The effect of the distance D between the Tx and the Rx and the effect of the path-loss exponent δ on the outage probability is illustrated in Figs. 2 and 3, respectively. As expected, the outage probability deteriorates as the value of D and(or) δ increase(s). In Fig. 2, the fading parameters are set to: $\alpha = 1.25$, $\mu = 1$, $\nu = 2$, $\delta = 2$, $k = 4$, and $\gamma_{th} = 2$ dB, whereas in Fig. 3 the values of the fading parameters are: $\alpha = 1.25$, $\mu = 1$, $\nu = 2$, $k = 4$, $D = 1500$ m, and $\gamma_{th} = 2$ dB

In Figs. 4 and 5, the performance of the average BER for coherent BPSK is analyzed. Figure 4 illustrates the influence of the fading parameter μ on the average BER, whereas Fig. 5 plots the impact of the scaling parameter ν on the average BER. It is clear from Fig. 4 that as the value of μ increases (while other parameters are fixed, i.e., $\alpha = 0.625$, $\nu = 3$, $\delta = 2$, $k = 4$, and $D = 1500$ m), the average BER decreases. This can be interpreted as follows. As the value of μ increases, the number of multi-path at the receiver side increases. As a results the received average SNR increases, and therefore the system

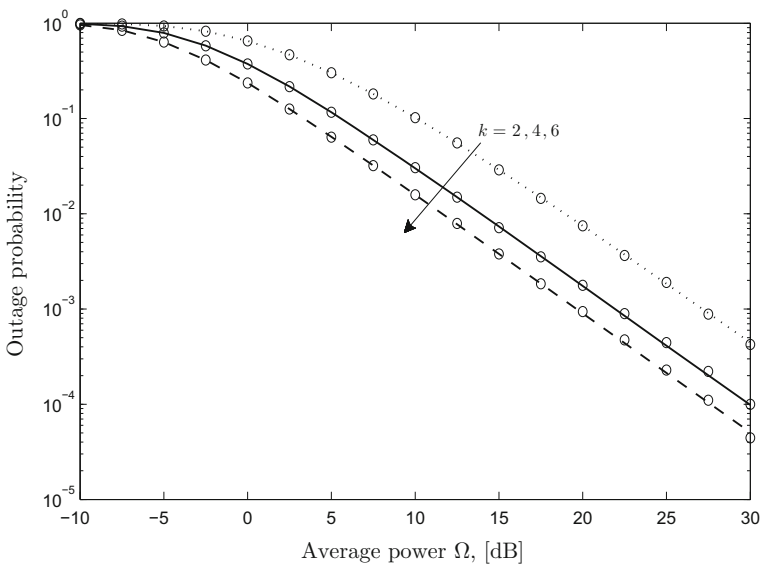


Fig. 1 Outage probability. $\alpha = 1.25$, $\mu = 1$, $\nu = 2$, $\delta = 2$, $D = 1500$ m, $\gamma_{th} = 2$ dB. Circle marks: Monte-Carlo simulations

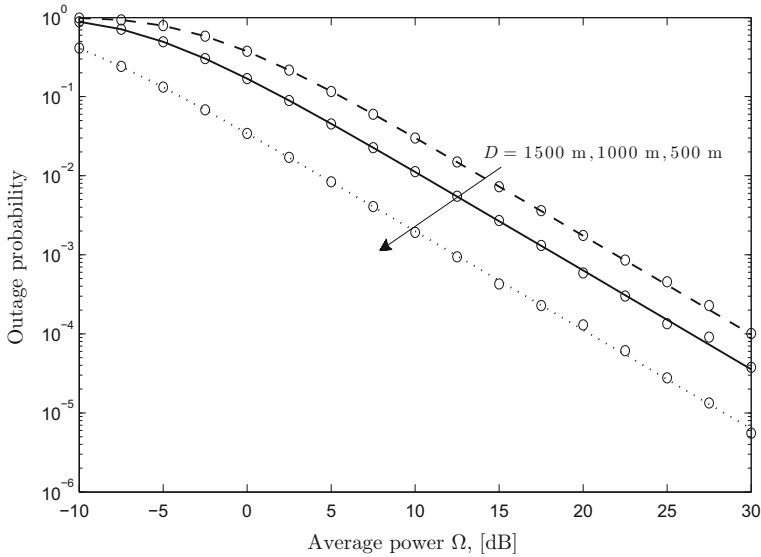


Fig. 2 Outage probability. $\alpha = 1.25, \mu = 1, \nu = 2, \delta = 2, k = 4, \gamma_{th} = 2$ dB. Circle marks: Monte-Carlo simulations

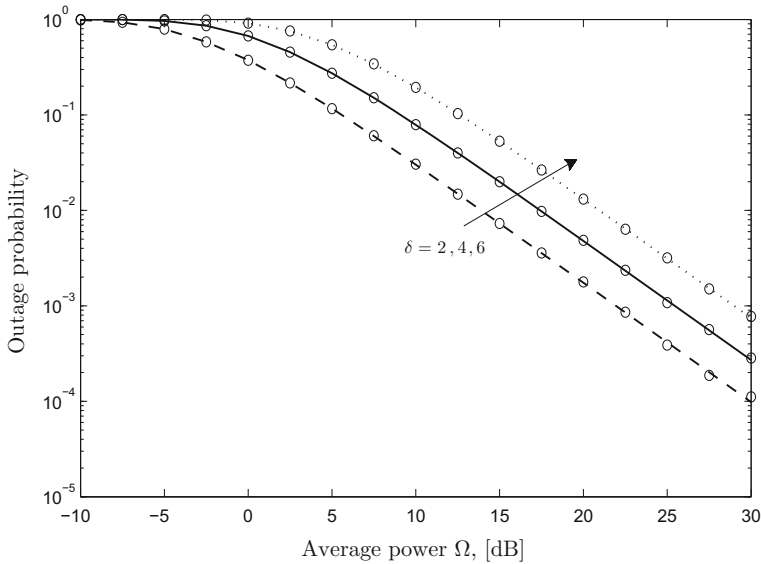


Fig. 3 Outage probability. $\alpha = 1.25, \mu = 1, \nu = 2, k = 4, D = 1500$ m, $\gamma_{th} = 2$ dB. Circle marks: Monte-Carlo simulations

performance improves. In the same context, as the value of the scale parameter ν increases (when other parameters are fixed: i.e., $\alpha = 1.375, \mu = 1, \delta = 2, k = 4$, and $D = 1500$ m), the system performances improves.

The system performance, in terms of the average channel capacity, is studied in Figs. 6, 7, 8 and 9. In Figs. 6 and 7, as the value of the fading parameters α and(or) μ

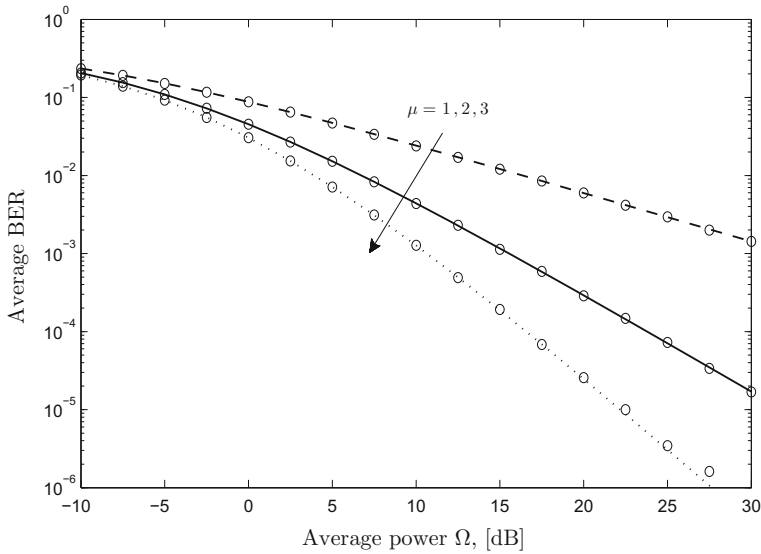


Fig. 4 Average BER. $\alpha = 0.625, v = 3, \delta = 2, k = 4, D = 1500$ m. Circle marks: Monte-Carlo simulations

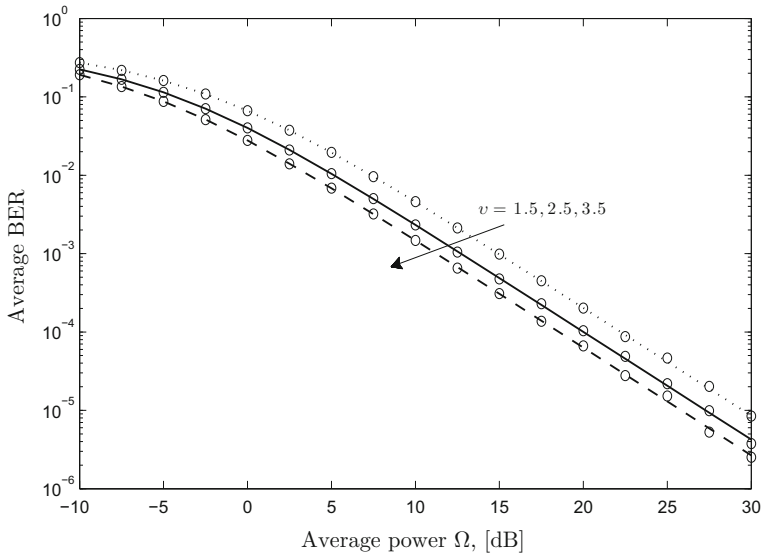


Fig. 5 Average BER. $\alpha = 1.375, \mu = 1, \delta = 2, k = 4, D = 1500$ m. Circle marks: Monte-Carlo simulations

increases, the average channel capacity improves. However, this improvement is more pronounced when the value of α increases compared with μ when other parameters are fixed and set to $v = 2, \delta = 4, k = 5$, and $D = 1500$ m.

Figure 8 shows the impact of the shape parameter k on the average channel capacity. The values of the other parameters are set to: $\alpha = 1.5, \mu = 2, v = 2, \delta = 4$, and $D = 1500$ m. One can note that as k increases, the average channel capacity increases. On

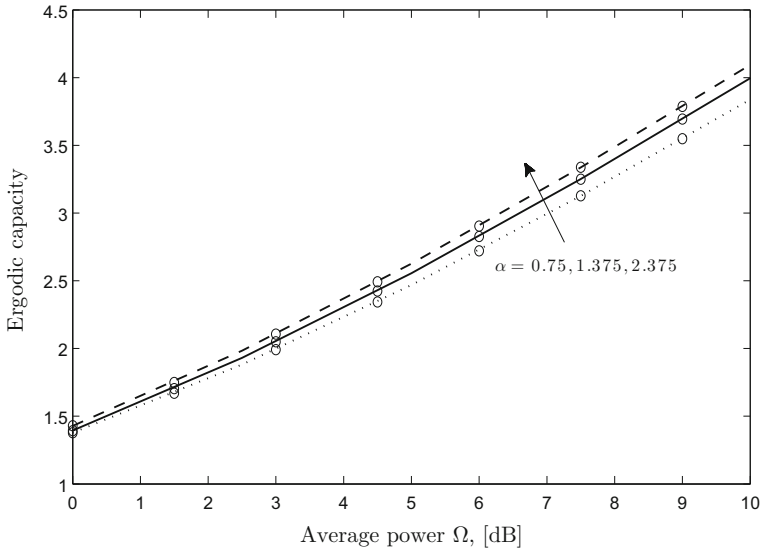


Fig. 6 Average channel capacity. $\mu = 2, \nu = 2, \delta = 4, k = 5, D = 1500$ m. Circle marks: Monte-Carlo simulations

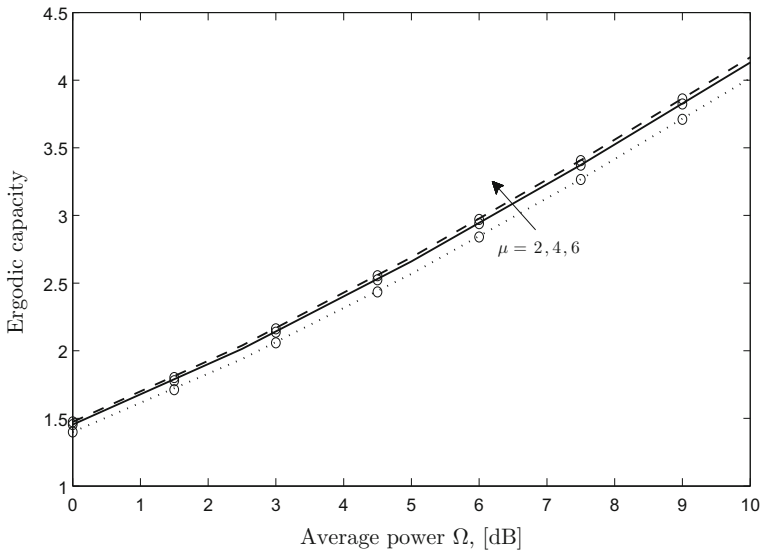


Fig. 7 Average channel capacity. $\alpha = 1.5, \nu = 2, \delta = 4, k = 5, D = 1500$ m. Circle marks: Monte-Carlo simulations

the other hand, Fig. 9 shows that the average capacity decreases as the value of the path-loss exponent δ increases. In Fig. 9, the value of the other parameters are set to: $\alpha = 1.25, \mu = 2, \nu = 2, k = 6,$ and $D = 1500$ m.

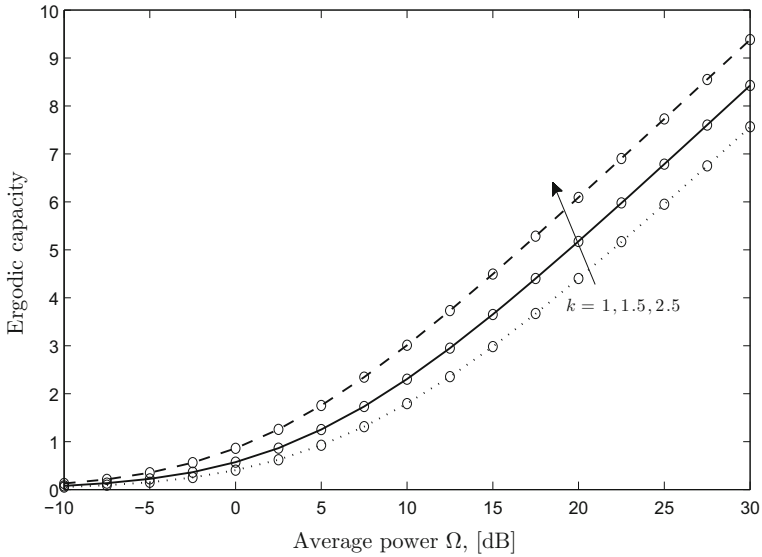


Fig. 8 Average channel capacity. $\alpha = 1.5, \mu = 2, \nu = 2, \delta = 4, D = 1500$ m. Circle marks: Monte-Carlo simulations

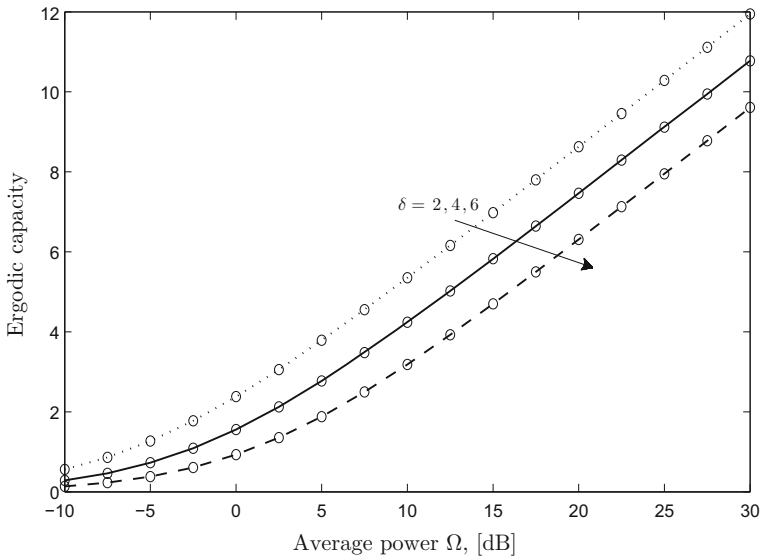


Fig. 9 Average channel capacity. $\alpha = 1.25, \mu = 2, \nu = 2, k = 6, D = 1500$ m. Circle marks: Monte-Carlo simulations

5 Conclusion

In this paper, we have analyzed a wireless communication system that operates over the composite $\alpha-\mu/\text{gamma}$ fading channels. Numerical results demonstrated that the system performance improves as the fading parameters, i.e., α, μ , the scale parameter ν , and the

shape parameter k increase. On the other hand, the system performance degrades as the values of the distance D (the distance between the Tx and Rx) and the path-loss exponent δ increase.

References

1. Simon, M. K., & Alouini, M. (2005). *Digital communication over fading channels* (2nd ed.). New York: Wiley.
2. Hansen, F., & Finn, M. I. (1977). Mobile fading—Rayleigh and lognormal superimposed. *IEEE Transactions on Vehicular Technology*, 26(4), 332–335.
3. Raghavan, R. S. (1991). A model for spatially correlated radar clutter. *IEEE Aerospace and Electronic Systems*, 27(2), 268–275.
4. Abdi, A., & Kaveh, M. (1998). k distribution: An appropriate substitute for Rayleigh-lognormal distribution in fading shadowing wireless channels. *Electronics Letters*, 34(9), 851–852.
5. Yilmaz, F., & Alouini, M. (2010). A new simple model for composite fading channels: Second order statistics and channel capacity. In *Proceedings of the 2010 7th International Symposium on Wireless Communication Systems, ISWCS* (pp. 676–680)
6. Shankar, P. M. (2004). Error rates in generalized shadowed fading channels. *Wireless Personal Communications*, 28, 233–238.
7. Badarneh, O. S. (2015). Error rate analysis of m -ary phase shift keying in α - η - μ fading channels subject to additive Laplacian noise. *IEEE Communications Letters*, 19(7), 1253–1256.
8. Shankar, P. (2013). Maximal ratio combining (MRC) in shadowed fading channels in presence of shadowed fading cochannel interference (CCI). *Wireless Personal Communications*, 68(1), 15–25.
9. Lei, X., & Fan, P. (2010). On the error performance of M -ary modulation schemes on Rician–Nakagami fading channels. *Wireless Personal Communications*, 53(4), 591–602.
10. Kapucu, N., Bilim, M., & Develi, I. (2014). A closed-form MGF expression of instantaneous SNR for weibull fading channels. *Wireless Personal Communications*, 77(2), 1605–1613.
11. Lee, H. (2015). High-SNR approximate closed-form formulas for the average error probability of M -ary modulation schemes over Nakagami- q fading channels. In J. Park, Y. Pan, H.-C. Chao, & G. Yi (Eds.), *Ubiquitous Computing Application and Wireless Sensor, Series Lecture Notes in Electrical Engineering* (Vol. 331, pp. 11–22). Netherlands: Springer.
12. Miridakis, N. I. (2015). Performance analysis of EGC receivers over generalized- \mathcal{K} (\mathcal{K}_G) fading channels. *Wireless Personal Communications*, 80(1), 167–173.
13. Zhang, J., Matthaoui, M., Tan, Z., & Wang, H. (2012). Performance analysis of digital communication systems over composite η - μ /gamma fading channels. *IEEE Transactions on Vehicular Technology*, 61(7), 3114–3124.
14. Ansari, I. S., Yilmaz, F., Alouini, M.-S., & Kucur, O. (2014). New results on the sum of gamma random variates with application to the performance of wireless communication systems over Nakagami- m fading channels. *Transactions on Emerging Telecommunications Technologies*, doi:10.1002/ett.2912.
15. Stamenović, G., Panić, S. R., Stefanović, D. R. Č., & Stefanović, M. (2014). Performance analysis of wireless communication system in general fading environment subjected to shadowing and interference. *EURASIP Journal on Wireless Communications and Networking*, 2014, 1–8.
16. Sofotasios, P. C., & Freear, S. (2015). A generalized non-linear composite fading model. *CoRR*, arXiv:1505.03779.
17. Yacoub, M. D. (2002). The α - μ distribution: A general fading distribution. In *Proceedings of the IEEE PIMRC*, September 15–18, 2002, pp. 629–629.
18. Shankar, P. M. (2011). Statistical models for fading and shadowed fading channels in wireless systems: A pedagogical perspective. *Wireless Personal Communications*, 60(2), 191–213.
19. Prudnikov, A. P., Brychkov, Y. A., & Marichev, O. I. (1990). *Integrals and series: More special functions* (Vol. 3). New York: Gordon & Breach Science Publishers, Inc.
20. Kilbas, A., & Saigo, M. (2004). *H-transforms: Theory and applications (Analytical Method and Special Function)* (1st ed.). Boca Raton: CRC Press.
21. Gradshteyn, I. S., & Ryzhik, I. M. (2007). *Table of integrals, series, and products* (7th ed.). California: Academic Press.
22. Mathai, A., & Saxena, R. (1978). *The H-function with applications in statistics and other disciplines*. New Delhi: Wiley Eastern.

23. Nakagami, M. (1960). The m -distribution-a general formula of intensity distribution of rapid fading. In *Proceedings of the symposium statistical methods radio wave propagation* (pp. 3–36). New York, NY, USA.



Osamah S. Badarneh received his Ph.D. in Electrical Engineering from University of Quebec-ETS (Canada) in 2009. He was an Assistant Professor in the Department of Telecommunication Engineering at Yarmouk University, Jordan, from January 2010 to September 2012. In 2012 he joined the Department of Electrical Engineering at University of Tabuk, Saudi Arabia, where he is currently an Associate Professor. He is also serve as an adjunct professor at University of Quebec-ETS in the Department of Electrical Engineering since November 2013. His research interests focus on wireless communications and networking.